

NON-VOLTAGE-GATED CALCIUM CHANNELS IN SNAIL HEART VENTRICLE CELLS

By B. L. BREZDEN AND D. R. GARDNER

Ottawa-Carleton Institute of Biology, Carleton University, Ottawa, Ontario, Canada K1S 5B6

Accepted 2 December 1989

Summary

1. Two recently identified channel types in *Lymnaea stagnalis* heart muscle cells were shown to conduct Na^+ in the absence of extracellular Ca^{2+} . They did not appear to be 'voltage-gated' as they were not activated by voltage. Also, they remained active over a wide range of membrane potentials. However, they were weakly 'voltage-sensitive' as their activity usually tended to increase with depolarization. The weak voltage-sensitivity and similarity to other non-voltage-gated Ca^{2+} channels suggested that one or both of these channels may be receptor-operated Ca^{2+} channels.

2. One of the two channels had a slope conductance of 15 pS. The other appeared to have at least two subconductance states with slope conductances of 50 and 72 pS. Both these conductance states had very similar open dwell-time constants and identical reversal potentials. The open dwell-time constants of both conductance states were not affected by voltage, suggesting that the channels' weak voltage-sensitivity was mediated by one of the closed states.

3. With divalent cations in the patch pipette, non-voltage-gated Ba^{2+} and Ca^{2+} currents were also detected. The Ba^{2+} conductance (12 pS) was similar to the Ca^{2+} conductance (11 pS).

Introduction

Bolton (1979) and Weiss (1981) discussed the possibility that some calcium channels in cell membranes are not gated by a change in membrane voltage, but depend on the presence of an appropriate agonist for the channel to open, i.e. that they form a class of receptor-operated channels. Only a few examples of such single-ion channels have been discovered so far to support this possibility. These include the calcium channel in human lymphocytes which is activated by phytohaemagglutinin (Kuno *et al.* 1986); the calcium channel in rabbit smooth muscle activated by ATP (Benham and Tsien, 1987); the thrombin-activated calcium channel in human platelet membranes (Zschauer *et al.* 1988); and the inositol-1,4,5-trisphosphate-activated calcium channel in sarcoplasmic reticulum vesicles from canine aortic smooth muscle (Ehrlich and Watras, 1988). A non-

Key words: calcium channels, non-voltage-gated, snail, heart cells.

voltage-gated channel permeable to calcium and barium has also been reported in *Aplysia* neurone membrane fragments (Coyne *et al.* 1987). Previous experiments on *Lymnaea* heart ventricle muscle cells indicate that receptor-operated calcium channels might also exist in these cells (Gardner and Brezden, 1984).

Once appropriate dissociation conditions had been discovered for isolating the *Lymnaea* heart cells (Gardner and Brezden, 1990), we were able to reveal a suite of cationic channels that conduct sodium ions when extracellular (i.e. patch electrode) calcium ions were kept below $10\ \mu\text{mol l}^{-1}$ (Gardner and Brezden, 1990). Only one of these, a rarely observed low-conductance channel, showed voltage-dependent activation (VG channel). In contrast, a novel stretch-activated Na^+ -conducting channel (SAN channel) was also described. The SAN channel is different from the well-characterized, stretch-activated potassium-conducting (SAK) channel (Brezden *et al.* 1986; Sigurdson *et al.* 1987).

Two other channels, distinguished by different conductances, were labelled 'small-conductance' (SG) and 'large-conductance' (LG) channels. Unlike the VG channel, SG and LG channels were not activated by voltage steps (i.e. they were not voltage-gated), they were insensitive to stretch, were not activated by the dihydropyridine (DHP) agonist Bay K 8644, and were blocked by $10\ \mu\text{mol l}^{-1}\ \text{Ca}^{2+}$ or Cd^{2+} , or by $1.0\ \text{mmol l}^{-1}\ \text{Co}^{2+}$. These properties of SG and LG channels make them distinct from the L-type, voltage-gated, DHP-sensitive Ca^{2+} channel summarized by Tsien *et al.* (1988). Rather, SG and LG channels appear more similar to receptor-operated Ca^{2+} channels (Kuno *et al.* 1986; Benham and Tsien, 1987; Zschauer *et al.* 1988; Ehrlich and Watras, 1988). Non-voltage-gated Ba^{2+} and Ca^{2+} currents were also detected in *Lymnaea* ventricle cells (Gardner and Brezden, 1990).

We have now obtained sufficient single-channel current data to enable a more detailed description of the kinetic properties of these LG and SG channels and these divalent cation currents in *Lymnaea* heart muscle cells. We discuss the possibility that at least one of these channel currents may be due to Na^+ passing through a receptor-operated calcium channel.

Materials and methods

The procedures for isolating and patch-clamping *Lymnaea* heart ventricle cells have been described in detail elsewhere (Brezden *et al.* 1986; Gardner and Brezden, 1990). Briefly, cells were dissociated by enzymatic dispersion (trypsin and collagenase) in $0.5\ \text{mmol l}^{-1}\ \text{Ca}^{2+}$ Leibovitz's medium and plated onto cover glasses. Micropipettes were pulled from thick-walled Corning 7052 (Kovar) glass. The tips were coated with Sylgard 184 elastomer (Dow Corning) and were heavily fire-polished. Channel currents were amplified with a List EPC-7 patch-clamp amplifier (Medical Systems Corp.). The data were recorded at 10 kHz on video cassette tape using a digital recorder (Instrutech VR-10). Data were filtered at 1–4 kHz (front panel setting) with four-pole Bessel filters, and subsequently processed and analysed with the pCLAMP program (version 4.5, Axon Instru

Table 1. The dissociation media and pipette solutions

Salt/Additive	Concentration (mmol l ⁻¹)				
	Low-Ca ²⁺ Leibovitz's medium	Pipette solutions			
		Normal	0Ca ²⁺ /0Mg ²⁺	50 mmol l ⁻¹ Ba ²⁺	50 mmol l ⁻¹ Ca ²⁺
NaCl	50.0	50.0	59.0	0	0
KCl	1.6	1.6	0	0	0
MgCl ₂	2.0	2.0	0	0	0
CaCl ₂	0.5	3.5	0	0	50.0
BaCl ₂	0	0	0	50.0	0
BDAC*	4.5	0	0	0	0
Hepes†	5.0	5.0	5.0	5.0	5.0
EGTA	0	0	1.0	0	0
Leibovitz's medium	33 %	0	0	0	0
Glucose	1.33 %	0	0	0	0
Foetal calf serum	1.33 %	0	0	0	0
Gentamycin	66 µg ml ⁻¹	0	0	0	0

* BDAC = bis(2-hydroxyethyl) dimethyl ammonium chloride (substituted for Ca²⁺).

† pH adjusted to 7.6 with NaOH.

The Ca²⁺ concentration of the 0Ca²⁺ saline was calculated as 3.2 nmol l⁻¹ using the dissociation constant of Owen (1976).

ments, Inc.). The analysis, fitting procedures and statistical tests employed are described by Sigurdson *et al.* (1987).

To ensure a very low Ca²⁺ concentration in the pipette, 1 mmol l⁻¹ EGTA was added to nominally zero-Ca²⁺ saline. Using the dissociation constant of Owen (1976) and the maximum residual Ca²⁺ content of the NaCl, the calculated Ca²⁺ concentration in the 'Ca²⁺-free' saline was 3.2 nmol l⁻¹. The pipette and bath saline compositions are given in Table 1. To avoid entry of bath saline into the pipette tip, positive pressure was maintained in the pipette until the tip came in contact with the cell membrane. Unless otherwise stated all values are presented as mean ± s.d.

Results

The single-channel currents described below, whether carried by Na⁺, Ca²⁺ or Ba²⁺, were labile. Channel activity either stopped abruptly, or tapered off at various rates, disappearing within a few seconds to a few minutes of seal formation. In most cases channel activity lasted for only a few seconds after seal formation; only on rare occasions did channel activity persist for more than 10 min. When activity ceased, the channels could never be re-activated by depolarizing voltage steps (see also Gardner and Brezden, 1990).

Estimates of the potential difference across the membrane patch (V_m) were

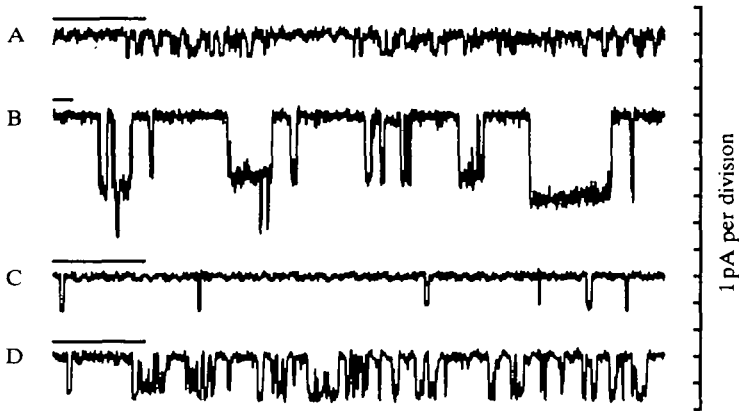


Fig. 1. Ion channel currents in *Lymnaea stagnalis* heart ventricle cells. Records A, B and D are from patches which initially exhibited multiple openings. As the experiments progressed, one or more of these channels usually ceased conducting. (A) Small inward Na^+ currents (SG channel). $V_m = -60$ mV. (B) Large inward Na^+ currents (LG channel). $V_m = -60$ mV. (C) Inward Ca^{2+} currents (CaP channel). $V_m = -60$ mV. (D) Inward Ba^{2+} currents (BaP channel). $V_m = -70$ mV. Horizontal scale bars, 50 ms.

based on the data of Brezden *et al.* (1986), who found the resting potential of isolated *Lymnaea stagnalis* heart ventricle cells to be -60 mV. Thus $V_m = (-60 - V_p)$ mV, where V_p is the pipette potential. All data are from cell-attached patches, and voltages are given as V_m .

The small-conductance channel

The small-conductance (SG) channel (Fig. 1A) was detected in only about 10% of the patches. It was usually characterized by infrequent bursts of activity separated by long intervals of inactivity, but occasionally remained very active for several minutes. The SG currents, which were -1.0 ± 0.2 pA in amplitude at a V_m of -60 mV (Fig. 2), were detected at membrane potentials between -100 and -40 mV. However, because of their small size, they could not be accurately measured at membrane potentials more positive than -40 mV, where the signal-to-noise ratio was poor. The slope conductance was 15 pS, and the reversal potential, determined by extrapolating the current/voltage curve (assuming linearity), was about -10 mV (Fig. 3). This channel usually became more active at depolarized potentials. In one patch, for example, the probability of a channel being open (P_o) was 0.18 at a membrane potential of -60 mV and 0.25 at -50 mV.

The open dwell-time distribution was best fitted by one exponential term, suggesting that this channel has a single open state. The open dwell-time constant, τ_o , was 1.0 ± 0.05 ms (\pm s.e.) at a membrane potential of -60 mV (Fig. 4). It was insensitive to voltage, ranging in a random fashion from 0.9 to 1.2 ms at membrane potentials between -40 and -100 mV (data not shown, $N=5$ patches).

Closed dwell-times, measured only within clearly defined bursts where n

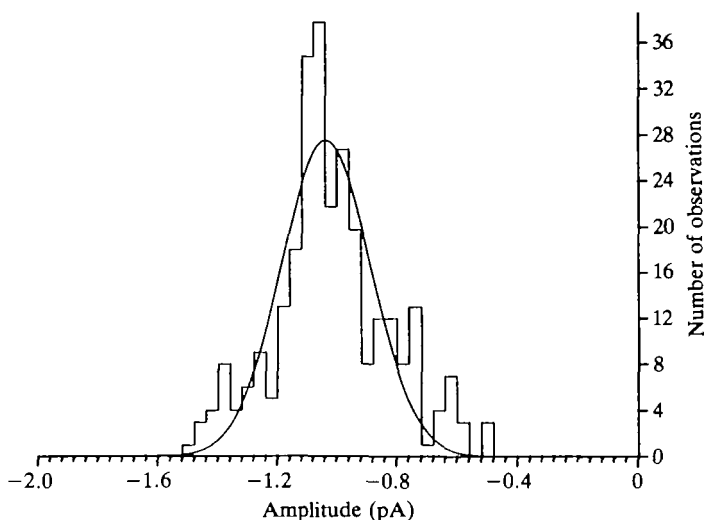


Fig. 2. Amplitude distribution of the SG channel currents. Single Gaussian fit. Mean amplitude = -1.0 ± 0.2 pA (\pm s.d.). Data are from a representative patch.

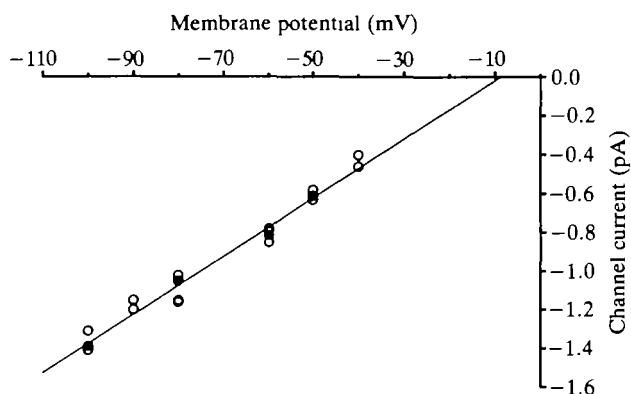


Fig. 3. Current/voltage relationship of the SG channel currents. The closed circles are data from a single patch. The open circles are data from four other patches (three cells). Slope conductance = 15 pS.

superimposed openings were observed, were best fitted by two exponential terms with time constants of 0.3 ± 0.02 ms (\pm s.e.) and 1.8 ± 0.2 ms (\pm s.e.) ($V_m = -60$ mV) (Fig. 5). As the SG bursts were infrequent, the closed times between bursts were not included in the analysis because too few data points were available.

The large-conductance channel

The large-conductance (LG) channel (Fig. 1B) was the most readily detected. It

was also more persistent than the SG channel, occasionally remaining active for many minutes. LG channel currents were detected at membrane potentials between -110 and -40 mV. Events having different current amplitudes, but indistinguishable kinetics, were often observed. The ratio of the smaller to the larger amplitude at $V_m = -60$ mV was always about 2:3. In a representative patch, for example, the mean amplitudes were -2.3 ± 0.3 pA and -3.2 ± 0.2 pA (Fig. 6).

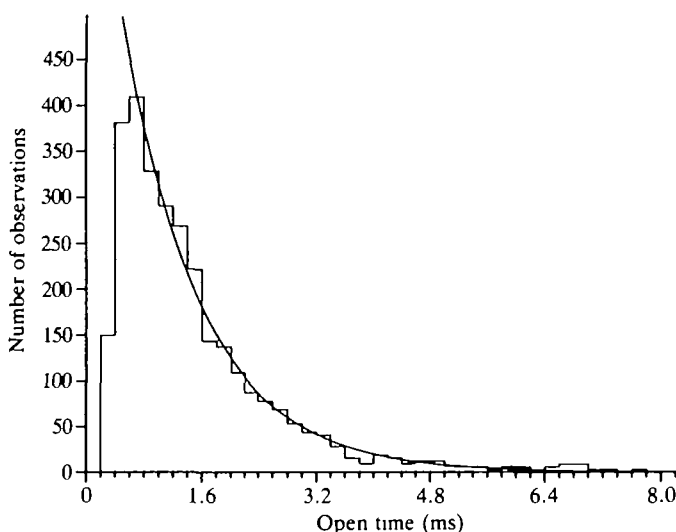


Fig. 4. Open dwell-time distribution of the SG channel. $\tau_o = 1.0 \pm 0.05$ ms (\pm s.e.). $V_m = -60$ mV. Data from four patches (three cells). Filter frequency = 2 kHz.

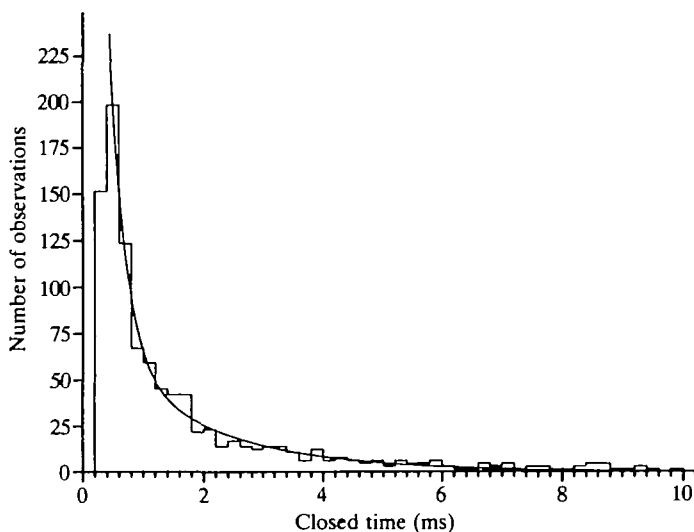


Fig. 5. Intraburst closed dwell-time distribution of the SG channel. $\tau_{c1} = 0.3 \pm 0.02$ ms. $\tau_{c2} = 1.8 \pm 0.2$ ms (\pm s.e.). $V_m = -60$ mV. Data from eight patches (eight cells). Filter frequency = 2 kHz.

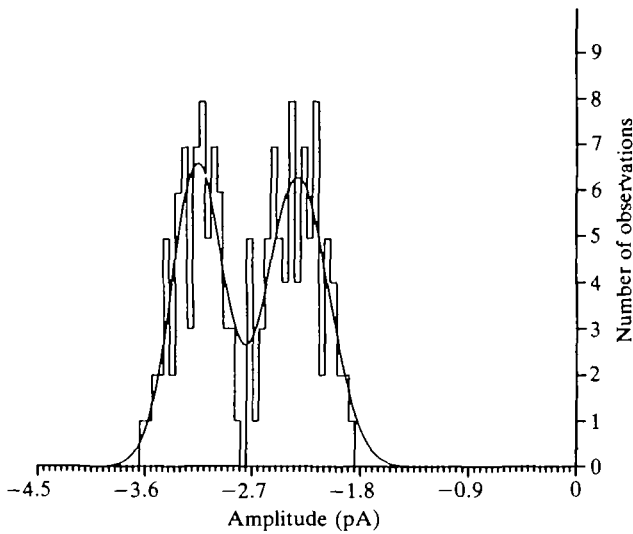


Fig. 6. Amplitude distribution of the LG channel currents. Double Gaussian fit. Mean amplitudes = -2.3 ± 0.3 and -3.2 ± 0.2 pA (\pm s.d.). $V_m = -60$ mV. Data are from a representative patch.

The open dwell-times for events of both amplitudes at $V_m = -60$ mV were best fitted by the sum of two exponential terms. The faster time constant, τ_{o1} , ranged from 0.2 to 0.6 ms for events of both amplitudes. The slower time constant, τ_{o2} , ranged from 1.4 to 2.8 ms for the smaller-amplitude events and 1.6 to 2.6 ms for the larger-amplitude events ($N=7$ patches). The combined open dwell-time data from events of both amplitudes at $V_m = -60$ mV gave $\tau_{o1} = 0.5 \pm 0.04$ ms (\pm s.e.) and $\tau_{o2} = 1.8 \pm 0.6$ ms (\pm s.e.) (Fig. 7).

Direct transitions from one amplitude to the other suggest that these events reflect different subconductance states of the same channel (Fig. 8). These transitions could not be attributed to the closings of a superimposed, smaller-amplitude channel because discrete, unitary events with the required amplitude of about -1 pA were absent from the patches where such transitions were observed. The slope conductance of the higher conductance state was 72 pS, and for the lower state 50 pS (Fig. 9). The extrapolated reversal potentials for both subconductances were nearly identical at about -20 mV. Brief (1–5 ms), discrete events with a larger amplitude of -5 to -6 pA at $V_m = -60$ mV were often observed (not shown). Whether these events represented a third subconductance state of the LG channel or whether they belonged to a different channel altogether could not be determined.

Channel openings usually appeared in closely spaced bursts at membrane potentials more positive than about -70 mV. Brief, single openings became more common at hyperpolarized potentials. Excluding bursts with superimposed openings from analysis, closed dwell-time data from seven patches ($V_m = -60$ mV), where at least two LG channels were present (see Sigurdson *et al.*

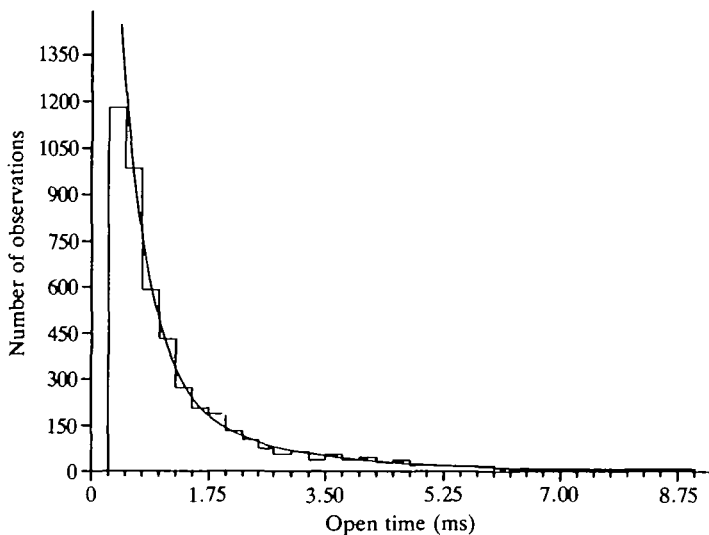


Fig. 7. Open dwell-time distribution of the LG channel. Combined data from small- and large-amplitude events, $\tau_{o1} = 0.5 \pm 0.04$ ms, $\tau_{o2} = 1.8 \pm 0.6$ ms (\pm s.e.). $V_m = -60$ mV. Filter frequency = 2 kHz.

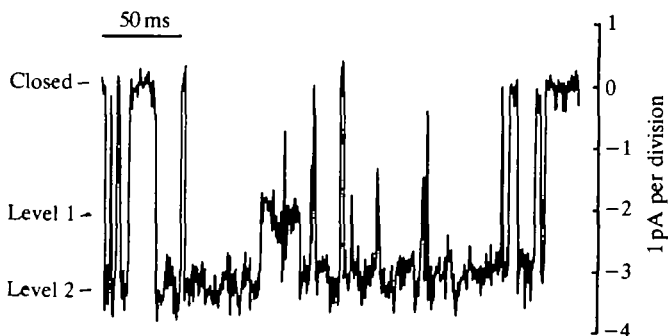


Fig. 8. Spontaneous transition of LG channel currents between two amplitudes. $V_m = -60$ mV.

1987), were best fitted by the sum of three exponential terms with closed dwell-time constants (τ_c) of $\tau_{c1} = 0.2 \pm 0.01$ ms (\pm s.e.), $\tau_{c2} = 1.4 \pm 0.17$ ms (\pm s.e.) and $\tau_{c3} = 10.5 \pm 1.7$ ms (\pm s.e.) (Fig. 10). In data from seven patches τ_{c1} ranged from 0.1 to 0.2 ms, τ_{c2} ranged from 1.3 to 3.0 ms and τ_{c3} , which showed the largest variation from patch to patch, ranged from 6.8 to 52.6 ms.

Like the SG channel, the LG channel activity also tended to increase with membrane depolarization, although there was no indication of voltage-induced gating. In one experiment, for example, the probability of the channel being open (P_o) decreased from 0.12 to 0.05 when the membrane potential was changed from

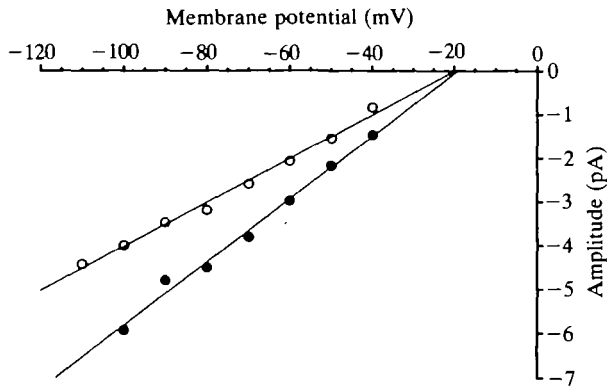


Fig. 9. Current/voltage relationship of the LG channel currents. Open circles, smaller subconductance; slope conductance = 50 pS. Closed circles, larger subconductance; slope conductance = 72 pS.

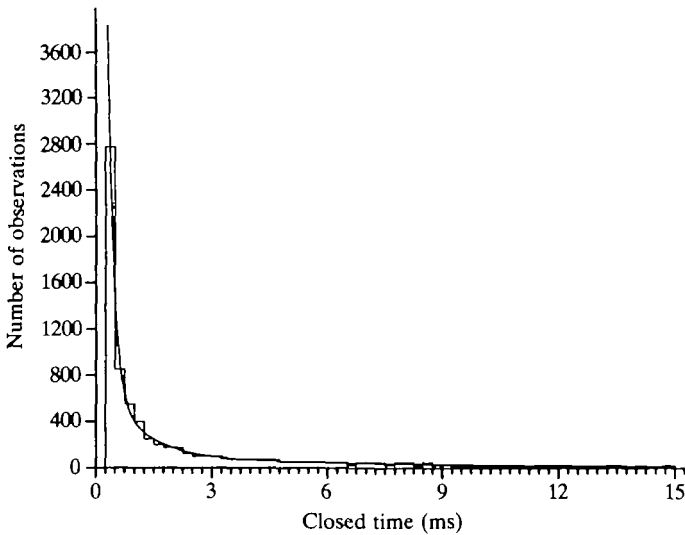


Fig. 10. Closed dwell-time distribution of the LG channel. $\tau_{c1} = 0.2 \pm 0.01$ ms, $\tau_{c2} = 1.4 \pm 0.17$ ms, $\tau_{c3} = 10.5 \pm 1.7$ ms (\pm s.e.). $V_m = -60$ mV. Data are from seven patches. Filter frequency = 4 kHz.

–40 to –100 mV. That this decrease was not due to the inevitable ‘run-down’ of the channel was confirmed by an increase in P_o to 0.09 when the membrane potential was subsequently raised to –70 mV. Although the actual P_o values varied considerably, the direct relationship between channel activity and membrane depolarization was observed in many patches.

Using data from a patch where both P_o and τ_o could be determined with confidence, it was found that neither τ_{o1} nor τ_{o2} was affected by changes in V_m

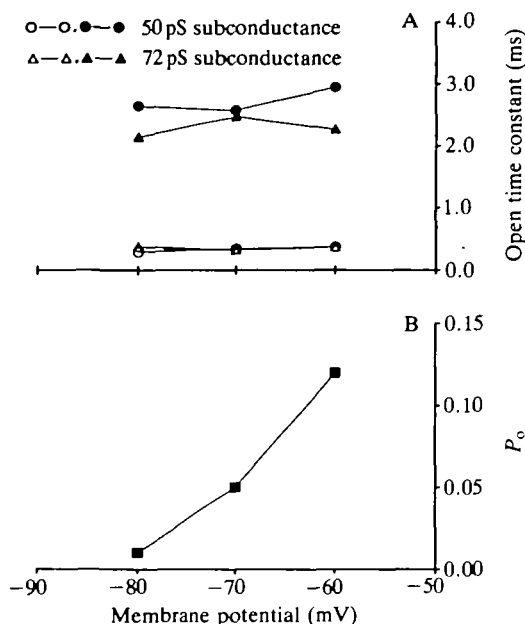


Fig. 11. The insensitivity of the LG channel open dwell-time constants during increased channel activity in response to membrane depolarization. $V_m = -60$ mV to -80 mV. (A) Effect of voltage on the fast (open symbols) and slow (closed symbols) components of the two subconductance states of the LG channel. Circles, 50 pS subconductance; triangles, 72 pS subconductance. (B) Effect of voltage on the probability of the channel being open.

(Fig. 11A), although the P_o for this same channel increased with increasing membrane depolarization (Fig. 11B).

Current reversals

Outward currents other than those of the SAK channel were generally not seen. Small outward currents of less than +1 pA were occasionally observed at membrane potentials between 0 and +40 mV, but these could not be ascribed to any one channel type since there was always more than one channel present in the patch. At other times the membrane patch was either quiescent, or the activity was dominated by outward SAK channel currents, which became spontaneously active at more depolarized potentials.

Divalent cation currents

With 50 mmol l⁻¹ Ca²⁺ in the pipette, inward unitary currents were detected at membrane potentials between -80 and -30 mV. These Ca²⁺-permeable (CaP) channel currents gave a mean current amplitude of -1.1 ± 0.1 pA at $V_m = -60$ mV. These events were very infrequent ($P_o < 0.01$), and disappeared within a short time of patch formation. Only short stretches of activity were detected, yielding sufficient data only for amplitude measurements. The slope

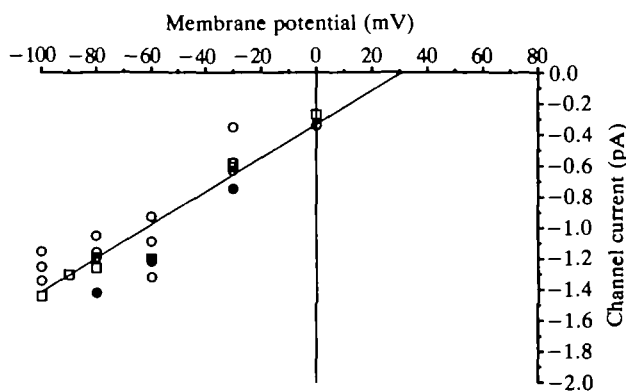


Fig. 12. Current/voltage relationship of Ca²⁺ currents. Filled circles are data from a single patch. Open squares are data from three patches on the same cell. Open circles are data from four patches on three different cells. Slope conductance = 11 pS.

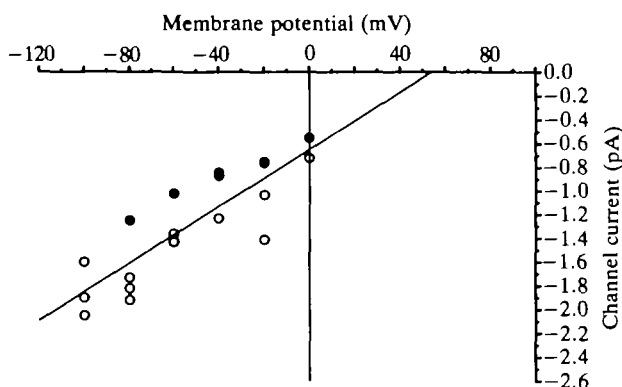


Fig. 13. Current/voltage relationship of Ba²⁺ currents. Closed circles are data from the same patch. Open circles are data from four different patches of three different cells. Slope conductance = 12 pS.

conductance for this channel was about 11 pS. Extrapolation, assuming linearity, gave a reversal potential of about +30 mV for these currents (Fig. 12). There were insufficient data to examine the kinetics of this channel.

With 50 mmol l⁻¹ Ba²⁺ in the pipette, the mean unitary current amplitude was -1.3 ± 0.2 pA at $V_m = -60$ mV. These Ba²⁺-permeable (BaP) channel currents, which did not appear to be voltage-gated, were detected at membrane potentials between -80 and -20 mV (Fig. 1D). The slope conductance was 12 pS. Extrapolation of the current/voltage curve (assuming linearity) shows a reversal potential of about +55 mV (Fig. 13). The open dwell-times were best fitted by a single exponential function with time constants ranging from 1.3 to 1.6 ms at $V_m = -60$ mV. Pooled data from six patches gave an open dwell-time constant of 1.4 ± 0.1 ms (\pm s.e.) (Fig. 14).

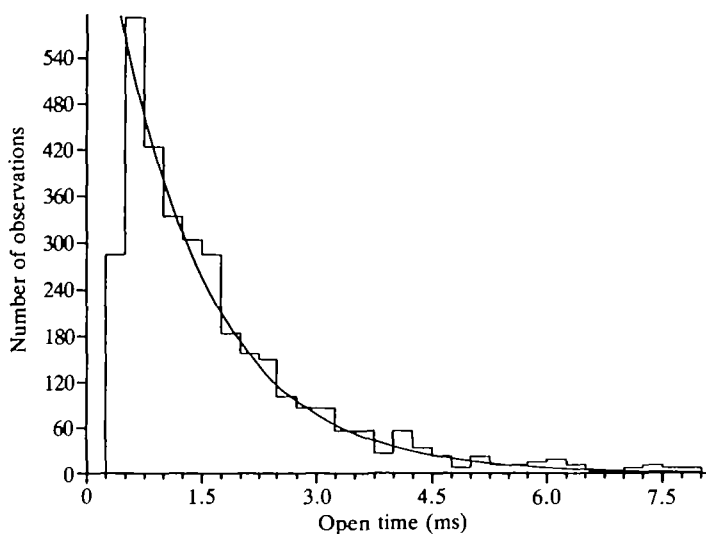


Fig. 14. Open dwell-time distribution of the Ba^{2+} -conducting channel. $\tau_o = 1.4 \pm 0.1$ ms (\pm s.e.). $V_m = -60$ mV. Data from six patches on four different cells. Filter frequency = 1 kHz.

Like the SG channel currents, the Ba^{2+} events appeared in infrequent bursts of activity. Closed dwell-times were measured only within those bursts where no superimposed openings were observed. They were best fitted by two exponential terms with time constants of 0.3 ± 0.02 (\pm s.e.) and 2.2 ± 0.3 ms (\pm s.e.) ($V_m = -60$ mV) (Fig. 15). The closed times between bursts were not included in the analysis because too few data points were available.

Discussion

We have previously described several new types of channel currents in *Lymnaea stagnalis* heart ventricle cells (Gardner and Brezden, 1990). In this paper we examine the properties of the SG, LG and divalent ion currents in greater detail.

In the absence of patch pipette Ca^{2+} , it is unlikely that either the SG or the LG current was due to Na^+ passing through SAK channels because inward LG channel and SG channel Na^+ currents, and outward SAK channel K^+ currents, were frequently active simultaneously in the same patch (Gardner and Brezden, 1990). Also, the currents detected with $50 \text{ mmol l}^{-1} \text{Ca}^{2+}$ or $50 \text{ mmol l}^{-1} \text{Ba}^{2+}$ in the pipette could not be due to the influx of a different cation species since only Ca^{2+} or Ba^{2+} (as Cl^- salts) and 5 mmol l^{-1} Hepes were present in the patch pipette. Neither could these currents, which were inward at $V_m = -60$ mV, have been due to an efflux of Cl^- because the reversal potentials were much more positive than the Cl^- equilibrium potential, which is close to the resting potential in these cells (Brezden and Gardner, 1984).

None of the channels described here appeared to be 'voltage-gated' since the

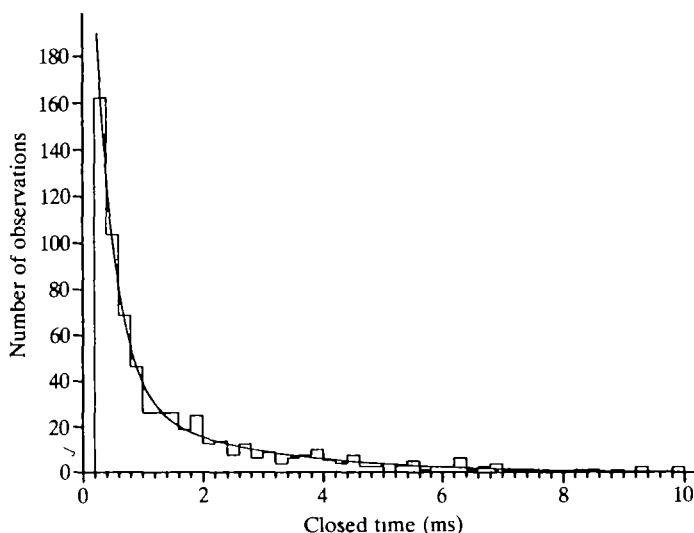


Fig. 15. Intraburst closed dwell-time distribution of the Ba²⁺-conducting channel. $\tau_{c1} = 0.3 \pm 0.02$ ms; $\tau_{c2} = 2.2 \pm 0.3$ ms (\pm s.e.). $V_m = -60$ mV. Data from one patch. Filter frequency = 4 kHz.

were not activated by voltage steps. However, both the SG and LG channels were 'voltage-sensitive' in that P_o often increased with membrane depolarization. The voltage-sensitivity of the LG channel, at least, would appear to be due to a reduction in one or more closed dwell-time constants, since the open dwell-time constants were not affected by a voltage change.

The BaP channel

The BaP channels in this study appear to be different from the Ba²⁺-permeable 'HP' channel recently found in *Lymnaea stagnalis* neurones (Yazejian and Byerly, 1989). Although both channels were weakly voltage-sensitive and neither was voltage-gated, the HP channel had a larger slope conductance (27 pS vs 12 pS for the BaP channel), and did not pass a detectable Na⁺ current in inside-out patches. However, as the HP channel was inactive in cell-attached patches (Yazejian and Byerly, 1989), it could not be determined whether the HP channels conducted Na⁺ in the intact cell. Whole-cell currents from *Lymnaea* neurones showed that 50 mmol l⁻¹ Na⁺ produced only a slightly greater current than 60 mmol l⁻¹ Ba²⁺, but this Na⁺ current could not be attributed to ion flux through the HP channel.

The lack of HP channel activity in cell-attached patches invites comparison with our own inability to detect Ca²⁺ or Ba²⁺ currents in *Lymnaea* heart cells which had been dissociated and incubated in medium containing 3.5 mmol l⁻¹ Ca²⁺ (Gardner and Brezden, 1990). However, the neuronal HP channel appears to be activated in the cell-attached patch configuration by an increase in the intracellular Ca²⁺ concentration, whereas our evidence suggests that the BaP and CaP channels are inactivated by high intracellular [Ca²⁺] (Gardner and Brezden, 1990).

Comparison of the SG channel Na⁺ currents with BaP channel Ba²⁺ currents

Several characteristics were common to both the unitary SG channel Na⁺ currents and the BaP channel Ba²⁺ currents. The Ba²⁺ currents were similar in appearance to the SG Na⁺ currents (cf. Fig. 1A and 1D). For both the SG and BaP channels, the open dwell-time distribution was described by a single exponential, while the distribution of the closed dwell-times within the bursts was described by two exponential terms. The activity of the BaP and SG channels was characterized by active stretches separated by relatively long intervals of low activity or inactivity (not evident in Fig. 1).

The reversal potential for the Na⁺ currents was considerably more negative than the reversal potential for the Ba²⁺ currents (-10 mV vs $+55$ mV). If SG and BaP are in fact the same channel, this suggests that the relative affinity of Na⁺ for the ion binding site(s) was lower than that of Ba²⁺. As a result, a counter-flux of K⁺ could more effectively shift the reversal potential for the Na⁺ current in the negative direction towards the K⁺ equilibrium potential (Hess *et al.* 1986). The data we have so far obtained for the CaP channel are also consistent with this view.

Also, ions with a lower affinity for the channel binding site(s) would be expected to have a higher throughput rate (higher conductance) because of a shorter dwell-time within the channel. If SG represented the same channel as BaP or CaP, it would be expected that a larger conductance would be seen with Na⁺ than with Ba²⁺ or Ca²⁺ as the charge carrier (Tsien *et al.* 1987). Our data are consistent with this expectation (15 pS for the SG currents, 11 pS for the CaP currents and 12 pS for the BaP currents).

LG channel subconductances

The LG channel is readily distinguished from the SG channel by its larger unitary current amplitude, and its very different kinetics (cf. Fig. 1A and Fig. 1B). Our evidence suggests that the LG channel may be able to assume at least two subconductance states, whereas the SG, BaP and CaP channels exhibited only a single amplitude level at any given membrane potential. Subconductance states have been described for L-type Ca²⁺ channels in vertebrate muscle cells (Pietrobon *et al.* 1988), and in reconstituted Ca²⁺- and Ba²⁺-permeable, non-voltage-gated channels from *Aplysia* neurones (Coyne *et al.* 1987).

In several respects, the LG channel resembles the Ca²⁺- and Ba²⁺-permeable channel in *Aplysia* neurones (Coyne *et al.* 1987). Neither channel was voltage-gated and both apparently can assume subconductance states. The open dwell-times of the two smaller subconductances of the *Aplysia* channel and the two subconductances of the *Lymnaea* LG channel were described by the sum of two exponential terms. In contrast, the *Aplysia* channel closed dwell-times are described by the sum of two exponential terms, whereas the *Lymnaea* LG channel closed dwell-times are best fitted by the sum of three exponential terms. The LG channel activity was often in the form of clearly defined bursts separated by relatively long interburst ('between burst') intervals. Therefore, it was possible to

measure with reasonable accuracy the intraburst ('within burst') closed dwell-times from patches which contained more than one channel. The influence of another channel on intraburst closed dwell-time measurements could be virtually eliminated by excluding from analysis those bursts with superimposed channel openings. In contrast, measurements of interburst closed dwell-times, where consecutive bursts may belong to different channels, are much more uncertain (Sigurdson *et al.* 1987). Given these considerations, the two fastest closed dwell-time constants, τ_{c1} and τ_{c2} , showed little variation from patch to patch. Therefore, they probably define the mean intraburst closed dwell-times where the measurement error is minimal. The slowest time constant, τ_{c3} , which showed the largest variation (ranging from 6.8 to 52.6 ms), probably reflects the interburst closed dwell-time, where the largest measurement error would be expected. Considerable variation in the slowest time constant is also likely to result from the observed decline of channel activity over time, which was not consistent from patch to patch.

The larger-amplitude events in the *Aplysia* channel were described by a single exponential term (Coyne *et al.* 1987). These latter events were very similar in appearance to the discrete large-amplitude events which we observed, but could not classify, in *Lymnaea* heart cell patches containing the LG channel. In contrast, Bay K 8644 had a marked effect on the *Aplysia* channel, whereas it had no discernible effect on the *Lymnaea* LG channel (Gardner and Brezden, 1990).

Channel identity

The following summarizes the evidence which suggests that the SG and LG channels may be Ca^{2+} channels: (1) the channels conduct Na^+ only in the absence of Ca^{2+} ; (2) the channels are blocked by very low concentrations ($10 \mu\text{mol l}^{-1}$) of Ca^{2+} (Gardner and Brezden, 1990); (3) the channel currents are blocked by Co^{2+} and Cd^{2+} , which are known Ca^{2+} -entry blockers in these cells (Gardner and Brezden, 1990); (4) Ca^{2+} and Ba^{2+} currents can be detected, showing that Ca^{2+} -permeable and Ba^{2+} -permeable channels *do* exist in *Lymnaea* heart ventricle cells; (5) the reversal potentials of the SG and LG Na^+ currents were much more negative than would be expected for a Na^+ -selective channel. This could be explained if Na^+ was passing through a symmetrical Ca^{2+} channel which also allowed K^+ to pass in the opposite direction (Reuter, 1983; Lee and Tsien, 1982). In this case, the inward Na^+ current would be offset by an outward K^+ current, since both ion types would permeate the channel.

Receptor-operated Ca^{2+} channels

The existence of receptor-operated channels was originally based primarily on indirect evidence (Bolton, 1979; Weiss, 1981). There are a few reports of non-voltage-gated, Ca^{2+} -conducting channels in molluscan cells (Chesnoy-Marchais, 1985; Coyne *et al.* 1987; Yazejian and Byerly, 1989). Although there is no strong evidence that these molluscan channels are receptor-operated, their weak voltage-sensitivity suggests that they may be either receptor-operated or gated *via* second

messengers. Recently, however, several voltage-independent, Ca^{2+} -conducting channels which are activated by a variety of agonist molecules have been reported for vertebrate cells. A Cd^{2+} -sensitive, Ba^{2+} -conducting channel in human T lymphocytes is activated by phytohaemagglutinin (Kuno *et al.* 1986). This channel is relatively non-selective for Ca^{2+} . An ATP-activated, Ca^{2+} -conducting channel has been found in rabbit smooth muscle cells (Benham and Tsien, 1987). These channels are insensitive to Cd^{2+} and also have a relatively low $\text{Ca}^{2+}/\text{Na}^{+}$ permeability ratio of 3:1. Thrombin-stimulated channels with a selectivity ratio for $\text{Ba}^{2+}/\text{Na}^{+}$ of 35:1 have been reported in human blood platelets (Zschauer *et al.* 1988). These channels have a Ba^{2+} slope conductance of 10 pS, are blocked by Ni^{2+} and are insensitive to dihydropyridines.

As the SG, LG, BaP and CaP channels do not appear to be voltage-gated, it is possible that some or all of them are the receptor-operated (or second-messenger-operated) Ca^{2+} channels that we concluded must exist from our studies on the mode of action of the molluscicide Frescon (Gardner and Brezden, 1984). This hypothesis has since been strengthened by our recent discovery that channel currents with similar properties to SG, LG, BaP and CaP currents can be activated by FMRFamide and related substances (B. L. Brezden, P. R. Benjamin and D. R. Gardner, in preparation).

DRG thanks the Natural Sciences and Engineering Research Council of Canada for an operating grant (A-4290).

References

- BENHAM, C. D. AND TSIEN, R. W. (1987). A novel receptor-operated Ca^{2+} -permeable channel activated by ATP in smooth muscle. *Nature, Lond.* **328**, 275–278.
- BOLTON, T. B. (1979). Mechanism of action of transmitters and other substances on smooth muscle. *Physiol. Rev.* **59**, 607–718.
- BREZDEN, B. L. AND GARDNER, D. R. (1984). The ionic basis of the resting potential in a cross-striated muscle of the aquatic snail *Lymnaea stagnalis*. *J. exp. Biol.* **108**, 305–314.
- BREZDEN, B. L., GARDNER, D. R. AND MORRIS, C. E. (1986). A potassium-selective channel in isolated *Lymnaea stagnalis* heart muscle cells. *J. exp. Biol.* **123**, 175–189.
- CHESNOY-MARCHAIS, D. (1985). Kinetic properties and selectivity of calcium-permeable single channels in *Aplysia* neurones. *J. Physiol., Lond.* **367**, 457–488.
- COYNE, M. D., DAGAN, D. AND LEVITAN, I. W. (1987). Calcium and barium permeable channels from *Aplysia* nervous system reconstituted in lipid bilayers. *J. Membrane Biol.* **97**, 205–213.
- EHRlich, B. E. AND WATRAS, J. (1988). Inositol 1,4,5-trisphosphate activates a channel from smooth muscle sarcoplasmic reticulum. *Nature, Lond.* **336**, 583–586.
- GARDNER, D. R. AND BREZDEN, B. L. (1984). Modification of Frescon action in *Lymnaea stagnalis* smooth and cross-striated muscles by agents that alter potential-dependent or receptor-operated calcium permeability. *Pest. Biochem. Physiol.* **21**, 403–411.
- GARDNER, D. R. AND BREZDEN, B. L. (1990). Single ion channels in snail ventricle heart cells. *Comp. Biochem. Physiol.* (in press).
- HESS, P., LANSMAN, J. B. AND TSIEN, R. W. (1986). Voltage and concentration dependence of single channel current in ventricular heart cells. *J. gen. Physiol.* **88**, 293–319.
- KUNO, M., GORONZY, J., WEYAND, C. M. AND GARDNER, P. (1986). Single-channel and whole-cell recordings of mitogen-regulated inward currents in human cloned helper T lymphocyte. *Nature, Lond.* **323**, 269–273.

- LEE, K. S. AND TSIEN, R. W. (1982). Reversal of current through calcium channels in dialysed single heart cells. *Nature, Lond.* **297**, 498–501.
- OWEN, J. D. (1976). The determination of the stability constant for calcium-EGTA. *Biochim. Biophys. Acta.* **451**, 321–325.
- PIETROBON, D., PROD'HOM, B. AND HESS, P. (1988). Conformational changes associated with ion permeation in L-type calcium channels. *Nature, Lond.* **333**, 373–376.
- REUTER, H. (1983). Calcium channel modulation by neurotransmitters, enzymes and drugs. *Nature, Lond.* **301**, 569–573.
- SIGURDSON, W. J., MORRIS, C. E., BREZDEN, B. L. AND GARDNER, D. R. (1987). Stretch-activation of a K^+ channel in molluscan heart cells. *J. exp. Biol.* **127**, 191–209.
- TSIEN, R. W., HESS, P., MCCLESKEY, E. W. AND ROSENBERG, R. L. (1987). Calcium channels: mechanism of selectivity, permeation, and block. *A. Rev. Biophys. biophys. Chem.* **16**, 265–290.
- TSIEN, R. W., LIPSCOMBE, D., MADISON, D. V., BLEY, K. R. AND FOX, A. P. (1988). Multiple types of neuronal calcium channels and their selective modulation. *Trends Neurosci.* **11**, 431–438.
- WEISS, G. B. (1981). Sites of action of calcium antagonists in vascular smooth muscle. In *New Perspectives in Calcium Antagonists* (ed. G. B. Weiss), pp. 83–94. Bethesda: American Physiological Society.
- YAZEJIAN, B. AND BYERLY, L. (1989). Voltage-independent barium-permeable channel activated in *Lymnaea* neurones by internal perfusion or patch excision. *J. Membrane Biol.* **107**, 63–75.
- ZSCHAUER, A., VAN BREEMEN, C., BÜHLER, F. R. AND NELSON, M. T. (1988). Calcium channels in thrombin-activated human platelet membrane. *Nature, Lond.* **334**, 703–705.